Research Article

Mediterranean Marine Science
Indexed in WoS (Web of Science, ISI Thomson) and SCOPUS
The journal is available on line at http://www.medit-mar-sc.net
DOI: http://dx.doi.org/10.12681/mms.27099

Ovarian dynamics, batch fecundity and spawning phenology of the Lessepsian migrant *Etrumeus golanii* DiBattista, Randall & Bowen, 2012 (Clupeidae: Dussumieriinae)

Stylianos SOMARAKIS[1], Maria GIANNOULAKI[1,2], Konstantinos MARKAKIS[1], Kostas TSIARAS[3], Eudoxia SCHISMENOU[1] and Panagiota PERISTERAKI[1]

[1] Hellenic Centre for Marine Research, Institute of Marine Biological Resources and Inland Waters, Thalassocosmos, Gournes, Crete, 71500 Greece
[2] Biology Department, University of Crete, Voutes University Campus, Heraklion, Crete, 70013 Greece
[3] Hellenic Centre for Marine Research, Institute of Oceanography, 46,7 km Athens-Sounio avenue, Anavyssos, Attiki, 19013 Greece

Corresponding author: somarak@hcmr.gr

Contributing Editor: Kostas STERGIOU

Received: 20 May 2021; Accepted: 27 July 2021; Published online: 2 September 2021

Abstract

Golani's round herring *Etrumeus golanii* is an Erythraean small pelagic fish (Lessepsian migrant) that entered the Mediterranean Sea through the Suez Canal. It has expanded its distribution from the eastern to the western Mediterranean with well-established local populations. We investigated basic aspects of its reproductive biology off the island of Crete (eastern Mediterranean) using ovarian histology and analysis of oocyte size-frequency distributions. The species exhibited a protracted breeding period (winter to early summer), with all ovaries examined during the main spawning season having markers of recent (postovulatory follicles, POFs) or imminent spawning (advanced oocyte batch in germinal vesicle migration or hydration). The advanced batch (AB) increased rapidly in size and was fully separated from the remainder, less developed oocytes in 95% of females with "old" POFs (POFs with signs of degeneration) and all females in final maturation. The growth of the subsequent batch (SB) was arrested at sizes <630 μm until full maturation of the AB. The mean diameter of hydrated oocytes ranged from 1181 to 1325 μm and relative batch fecundity was low ranging from 56 to 157 eggs g^{-1}. The simulation of a coupled hydrodynamic/biogeochemical model (POM/ERSEM) showed that *E. golanii* takes advantage of the seasonal cycle of planktonic production to reproduce, and exhibits monthly changes in batch fecundity that appear to be closely related with the seasonal cycle of mesozooplankton concentration.

Keywords: Round herring; reproduction; condition; Crete; eastern Mediterranean.

Introduction

The opening of the Suez Canal in the late 18th century led to a remarkable and continuing inflow of marine biota from the Red Sea into the Mediterranean (Lessepsian migrants), including more than 100 Indo-Pacific fishes (Galil *et al.*, 2021; Dr. Argyro Zenetos, personal communication, https://elnais.hcmr.gr/). Many of these non-indigenous Erythraean species are now established, and have proliferated and expanded from the east towards the central and western Mediterranean. Lessepsian migrants have been recognized as an important threat to native species, biodiversity and ecosystem functioning (Golani, 1998; Otero *et al.*, 2013; Katsanevakis *et al.*, 2014). Nevertheless, the establishment of certain non-indigenous species can also have positive impacts, particularly when they provide additional resources to local fisheries (e.g., Farrag *et al.*, 2014).

Etrumeus golanii, formerly known as *Etrumeus teres* (DeKay, 1842), is a small pelagic fish originally known from the northern Red Sea (DiBattista *et al*., 2012). In the Mediterranean, it was first recorded from Israel in 1961 and it subsequently spread across the sea to Morocco (Galil *et al.*, 2019; Tamsouri *et al.*, 2019; and references therein). An important population of Golani's round herring has already been established in the eastern Mediterranean and the species is commercially exploited in Egypt and Turkey (Farrag *et al.*, 2014; Çiftçi, & Bardakci, 2021). In Crete, it was first recorded in 2005 (Kasapidis *et al.*, 2007) and it is now regularly caught by commercial fisheries (Giannakaki *et al.*, 2018).

Given the possible expansion of fisheries for *E. golanii* in the Mediterranean Sea, the objectives of this study were to determine and describe basic aspects of its reproductive strategy, with a focus on spawning phenology, the pattern of oocyte development and fecundity enumeration. A previous study carried out in the Egyptian Mediterranean Sea showed that *E. golanii* is a multiple

spawner with a protracted spawning period (Osman *et al.*, 2011), as is the case with other *Etrumeus* species studied so far (Roel & Melo, 1990; Plaza *et al.*, 2007). Based on simulations of a coupled hydrodynamic/biogeochemical model, we show that *E. golanii* off Crete takes advantage of the seasonal cycle of plankton production, influenced by the seasonal variability of the thermocline and vertical mixing in the water column, and produces successive batches of large-sized pelagic eggs over a protracted spawning season.

Materials and Methods

Sample collection and processing

A total of 25 samples of round herrings were available for this study. They were collected opportunistically during the National onboard sampling program of the Cretan fishing fleets from 2016 to 2019 (Table 1). In 2016, most samples derived from a pilot boat seine (SB) fishery opened during the winter months (Table 1, Fig. 1). In 2017 and 2018, samples were primarily collected in autumn from purse seines (PS) and trammel nets (GTR). In 2019, samples covered the period from February to July and were mainly collected from purse seines and bottom trawls (OTB) (Table 1, Fig. 1). Finally, a pelagic trawl (PT) sample was obtained in December 2019 onboard the research vessel PHILIA in Heraklion bay (Table 1).

In most cases, especially in 2016-2018, fish samples were frozen at -20° C prior to laboratory analysis. However, on certain occasions (samples # 7, 8, 12, 16-22, 24-25), the fish were placed in iced sea-water onboard the fishing vessel (blast freezing) and transported immediately to the laboratory for further processing. These blast-frozen samples were used for ovarian histology and batch fecundity measurements (Table 1).

Processing of a sample in the laboratory consisted in measuring the total length (TL, mm) and weight (TW, 0.01g) of each individual and recording its sex (Table 1). Gonads were staged macroscopically, weighed (GW, 0.001g) and then preserved in 10% buffered formalin. A simplified macroscopic maturity scale was used (Supplementary Material, Table S1) based on the MEDITS maturity stages for Mediterranean bony fishes (Follesa & Carbonara, 2019). The length frequency distribution of collected fish is provided in the Supplementary Material (Fig. S1).

Histological analysis, oocyte size frequency distributions (OSFDs) and batch fecundity (BF) measurements

The ovaries of blast-frozen fish (n = 188) were subjected to histological analysis (Table 1). Pieces of ovarian tissue were embedded in glycol methacrylate resin (Technovit 7100, Heraeus Külzer, Germany), cut into 4-µm sections on a microtome, stained with methylene blue/azure II/basic fuchsin (Bennett *et al.*, 1976) and examined under a light microscope. Histological scoring included the developmental stage of the most advanced group of oocytes, the presence/degree of degeneration of postovulatory follicles (POFs) and the incidence/prevalence of follicular atresia (Hunter & Macewitz, 1985a,b).

The oocytes were assigned to stages according to Schismenou *et al.* (2012), i.e., PVO: primary growth oocytes; CA: oocytes with yolk vesicles or cortical alveoli formed; EVTO: early vitellogenic oocytes, with yolk granules not covering the entire cytoplasm; VTO: vitellogenic oocytes, with yolk granules all over the cytoplasm; GVM: oocytes in germinal vesicle migration; HYD: hydrated oocytes. Postovulatory follicles with a large-sized, thick and convoluted granulosa cell layer, and linearly arranged nuclei, were classified as "new" POFs. POFs with indications of degeneration were classified as "old" POFs (Hunter & Macewicz, 1985a). Concerning atresia, females were assigned to atretic states 0, 1, 2, and 3, having 0%, <50% and ≥ 50% of vitellogenic oocytes with α-atresia, and no vitellogenic oocytes but β-atresia, respectively (Hunter & Macewicz, 1985a, b).

Whole-mount analysis (Thorsen & Kjesbu, 2001; Ganias *et al.*, 2014a) was performed on fish collected in March-May (n = 60) using random pre-weighed subsamples from the ovaries (30 mg in non-hydrated and 60 mg

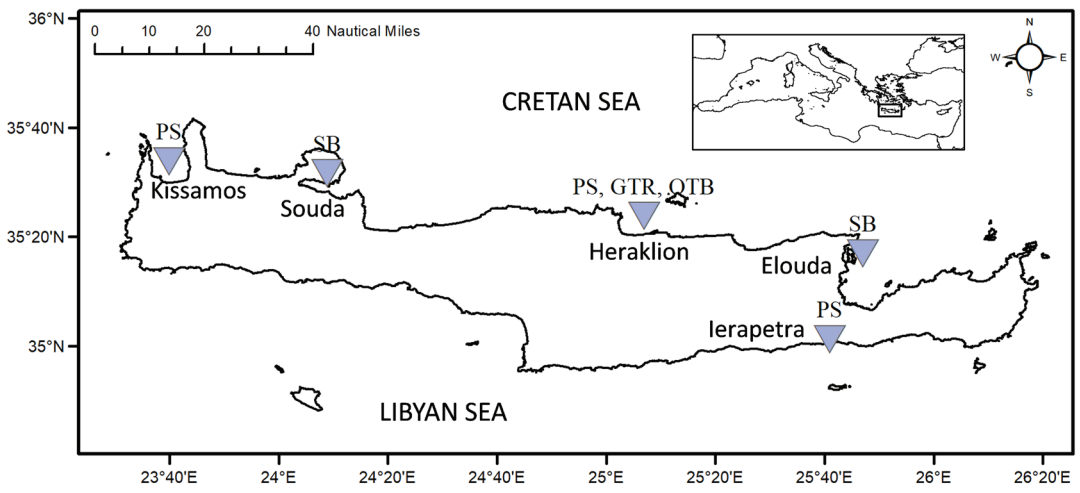

Fig. 1: Map of the study area showing the locations of sample collection and fishing gears used. SB: beach seine. PS: purse seine. GTR: trammel net. OTB: bottom trawl.

Table 1. Summarized information on samples collected and fish analyzed. N: number of fish. SB: beach seine. PS: purse seine. GTR: trammel net. OTB: bottom trawl. PT: pelagic trawl. TL: average total length (TL ranges in parentheses). N_F: number of females. N_M: number of males. N_U: number of fish with undetermined sex. F_H: number of females examined histologically. F_F: number of females with batch fecundity measurements. Areas of collection are shown in Figure 1.

Sample #	Date	Area of collection	Gear	Average bottom depth (m)	N	TL (mm)	N_F	N_M	N_U	F_H	F_F
1	30/1/2016	Elounda	SB	24	22	132 (106-169)	16	5	1		
2	5/2/2016	Souda	SB	26	19	144 (132-154)	13	6			
3	6/2/2016	Souda	SB	26	23	155 (136-207)	7	16			
4	12/2/2016	Souda	SB	29	33	166 (140-191)	26	7			
5	14/2/2016	Elounda	SB	37	24	142 (121-159)	15	9			
6	6/4/2016	Heraklion	PS	70	20	205 (147-229)	7	13			
7	31/5/2017	Heraklion	PS	65	18	244 (219-286)	10	8		10	7
8	29/11/2017	Heraklion	PS	109	20	207 (157-268)	14	6		14	
9	25/7/2018	Ierapetra	PS	64	29	235 (202-271)	22	6	1		
10	17/9/2018	Heraklion	PS	93	30	215 (191-238)	6	10	14		
11	18/9/2018	Ierapetra	PS	85	32	168 (121-203)	21	7	4		
12	18/9/2018	Ierapetra	PS	34	28	140 (131-157)	14	14		14	
13	24/9/2018	Heraklion	GTR	48	20	207 (186-224)	9		11		
14	24/10/2018	Ierapetra	PS	45	18	139 (129-157)			18		
15	8/11/2018	Heraklion	GTR	50	6	230 (217-240)	3	1	2		
16	25/2/2019	Souda	SB	23	30	156 (130-217)	16	14		16	16
17	28/3/2019	Souda	SB	15	3	119 (54-206)	3	1	5	3	3
18	11/4/2019	Heraklion	PS	63	28	205 (180-237)	28			28	13
19	13/5/2019	Heraklion	OTB	81	33	200 (164-240)	12	21		12	12
20	14/5/2019	Heraklion	OTB	95	23	184 (153-221)	4	19		4	3
21	16/5/2019	Heraklion	OTB	91	14	226 (194-250)	3	11		3	3
22	20/6/2019	Kissamos	PS	86	50	194 (169-230)	31	19		31	14
23	28/6/2019	Ierapetra	PS	75	30	219 (188-236)	3	27			
24	20/7/2019	Kissamos	PS	84	39	214 (185-241)	28	11		28	
25	15/12/2019	Heraklion	PT	59	100	148 (126-186)	47	53		25	
Total					692		358	284		188	71

in hydrated females). Previous studies have shown that *Etrumeus* ovaries are homogeneous with no significant differences in oocyte size and batch fecundity measurements between ovarian lobes and/or position (Plaza *et al.*, 2007; Nyuji & Takasuka, 2017). The methodology used for whole-mount analysis is described in Schismenou *et al.* (2012). Briefly, oocyte diameters were measured on images taken with a digital camera mounted on a microscope and using light from underneath. All oocytes >250 µm were measured semi-automatically using the open source ImageJ (http://rsb.info.nih.gov/ij/) with the plugin ObjectJ (http://simon.bio.uva.nl/objectj/). The volume of each oocyte was also calculated (assuming volume of a sphere).

Oocyte size frequency distributions (OSFDs) were constructed using both oocyte diameters and oocyte volumes, and with different options for histogram bin size (50 µm or 40 µm and 0.02 mm^3 0.01 mm^3 for diameter and volume, respectively) (Fig. 2). The rationale of using oocyte volume was that, being a three-dimensional indicator of size, it magnifies the growth differences between successive oocyte batches, allowing for better demonstration of ovarian dynamics and easier definition of the number of oocytes in the advanced batch (AB).

Batch fecundity (BF) was measured using the gravimetric method (Hunter *et al.*, 1985) in all GVM and HYD females (females in final maturation). Additionally, we measured BF in females with old POFs caught in March-May. Using the ovarian whole-mounts subsamples, we counted all oocytes forming the advanced oocyte batch (AB). Only females with a size hiatus, i.e. with the AB completely separated from the remaining oocytes, were used for BF measurements.

Gonadal and somatic condition

Seasonal changes in gonadal and somatic condition of males and females were analyzed with an "integrated" (*sensu* Plaza *et al.*, [2007]) approach, using general linear models (see also Somarakis *et al.*, [2012]; Geladakis *et al.*, [2018]; Gkanasos *et al.*, [2019]): Monthly least-square means (average monthly condition) were estimated by fitting the model:

$$\log(Y) = a + b_1 \times (\text{MONTH}) + b_2 \times (\text{YEAR}) + b_3 \times \log(X) + b_4 \times (\text{MONTH}) \times (\text{YEAR}) + b_5 \times (\text{MONTH}) \times \log(X) + b_6 \times (\text{YEAR}) \times \log(X)$$

where Y = gonad weight (GW) or gonad-free body weight (GFW), and X = GFW or total length (TL) for gonadal and somatic condition respectively,
MONTH = the month of sampling,
YEAR = the year of sampling, and
a, b_1, b_2, … are model coefficients.

Only significant terms ($p < 0.05$) were retained in the final models (backward stepwise selection) (Geladakis *et al.*, 2018; Gkanasos *et al.*, 2019). Females with hydrated ovaries were excluded from the analysis of gonadal condition because they were collected inconsistently. Their occasional presence in some samples inflated means and variances, which does not essentially reflect the respective variability in the reproductive activity of the fish (Plaza *et al.*, 2007; Ganias *et al.*, 2007).

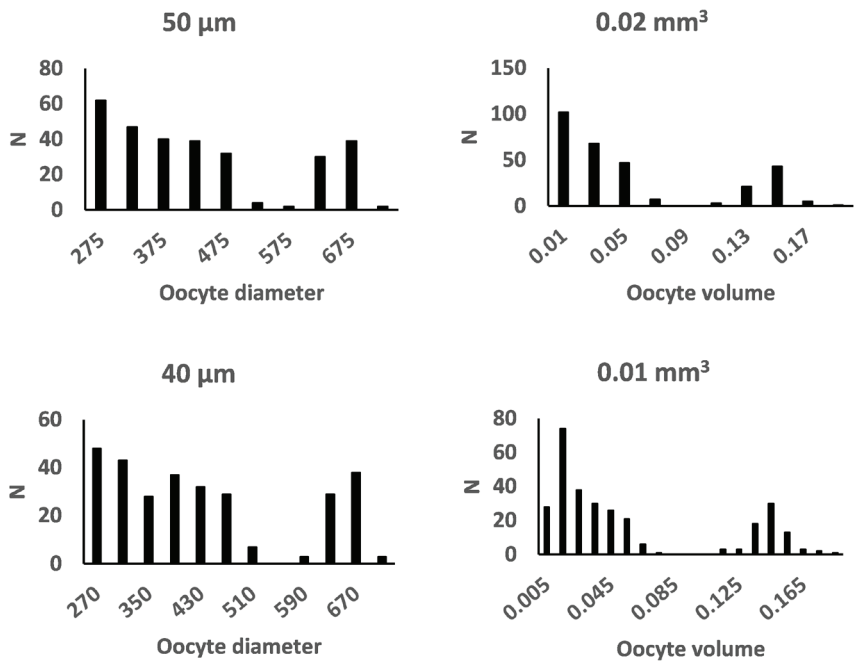

Fig. 2: Example of oocyte size frequency distributions (OSFDs) of a single individual *Etrumeus golanii* (a female with old post-ovulatory follicles). The four histograms were constructed using different options for oocyte size (diameter [left panel] vs volume [right panel]) and bin size (50 µm or 40 µm and 0.02 mm^3 or 0.01 mm^3 for diameter and volume respectively). The size hiatus between the advanced batch and the subsequent batch is more easily discernible when the bin size is narrower (lower panel) and/or volumes are used instead of diameters to construct the OSFD. N: number of oocytes.

Simulation of a hydrodynamic/biogeochemical model

In order to obtain a picture of the annual cycle of temperature and plankton productivity in the study area, and its relationship with spawning phenology and the temporal changes in fecundity and somatic condition of round herring, we used a simulation of a basin-scale Mediterranean coupled hydrodynamic-biogeochemical model (POM-ERSEM) (www.poseidon.hcmr.gr; Kalaroni *et al.*, 2020a, b). The model was setup and implemented with 1/20° (~5 Km) horizontal resolution for the period 2016-2019 (period of fish sampling), over an area surrounding the island of Crete (a rectangle defined by the coordinates 35.66667° N, 23.50000° E and 34.83333° N, 26.50000° E). The model outputs, namely, sea surface temperature (SST), near-surface Chl-α, and mesozooplankton concentration (0 - 100m) were averaged on a monthly basis. More details and the monthly time series of simulated parameters (Fig. S2) are provided in the Supplementary Material.

Results

Maturity

A total of 692 fish (358 females and 284 males) were available for this study. The samples covered all months of the year, except August, and fish lengths ranged from 106 to 286 mm (Table 1, Supplementary Material, Fig. S1). In September, all gonads examined were macroscopically classified as resting/virgin. Fish caught in October had very small, presumably virgin, gonads and their sex could not be identified macroscopically. Ovarian histology of 14 females caught in September (Table 2) confirmed that oocytes in early autumn were at the primary growth (PVO) phase (Fig. 3A). For samples collected in November/December, the gonads were macroscopically classified as resting/virgin, with the exception of few fish that were assigned to the recovering stage, and 3 females caught in November 2017 that were classified as developing (presence of opaque oocytes in the ovaries). The microscopic examination (Table 2) confirmed the macroscopic classification. Based on the developmental stage of the most advanced group of oocytes (Table 2), 3 out of the 14 females examined in November 2017 were classified as PVO, 8 as CA (Fig. 3B) and 3 as VTO (Fig. 3C). The latter included a fish that had recently spawned (with new POFs present in the ovary), implying that spawning may start as early as late autumn in some fish/years. In December, the ovaries examined were at the PVO and CA stages (Table 2).

All fish (>118 mm) caught in January-May were macroscopically classified as developing or ripe, except for 2 small individuals (106 - 107 mm) with undeveloped gonads and unidentifiable sex. The histological analysis revealed that, from February to May, all females were spawning capable (*sensu* Brown-Peterson *et al.*, 2011) (Table 2) with ovaries containing markers of either imminent (migratory nucleus [GVM] or hydrated [HYD] oocytes, Fig. 4A and 4B) or recent spawning (new or old POFs; Fig. 4C and 4D), or both (Table 2). No atretic follicles were observed in the histological sections from February-May. The first signs of atresia were observed in June (Table 2), with 4 out of the 31 females examined assigned to atretic states 2 (Fig. 3D) and 3. In July, spawning

Table 2. Results of histological scoring. Samples are sorted by month and day (September to July). Time: time at end of fishing haul. PVO: previtellogenic. CA: cortical alveoli. VTO: vitellogenic. GVM: germinal vesicle migration. HYD: Hydrated. POFs: postovulatory follicles. Atr-1 to Atr-3: atretic states (see text for explanations).

Sample #	Date	Time	PVO	CA	VTO	GVM	HYD	VTO + new POFs	VTO + old POFs	GVM + old POFs	HYD + old POFs	Atr-1	Atr-2	Atr-3
12	18/9/2018	17:16	14											
8	29/11/2017	21:50	3	8	2			1						
25	15/12/2019	16:12	10	15										
16	25/2/2019	19:22					5			7	4			
17	28/3/2019	19:07				2			1					
18	11/4/2019	01:40						15	13					
19	13/5/2019	21:25					10			1	1			
20	14/5/2019	21:12					1		3					
21	16/5/2019	20:45					3							
7	31/5/2017	01:45				4		3	2	1				
22	20/6/2019	03:05				9			12	5		1	3	1
24	20/7/2019	02:23	17										1	10
Total			44	23	2	15	19	19	31	14	5	1	4	11

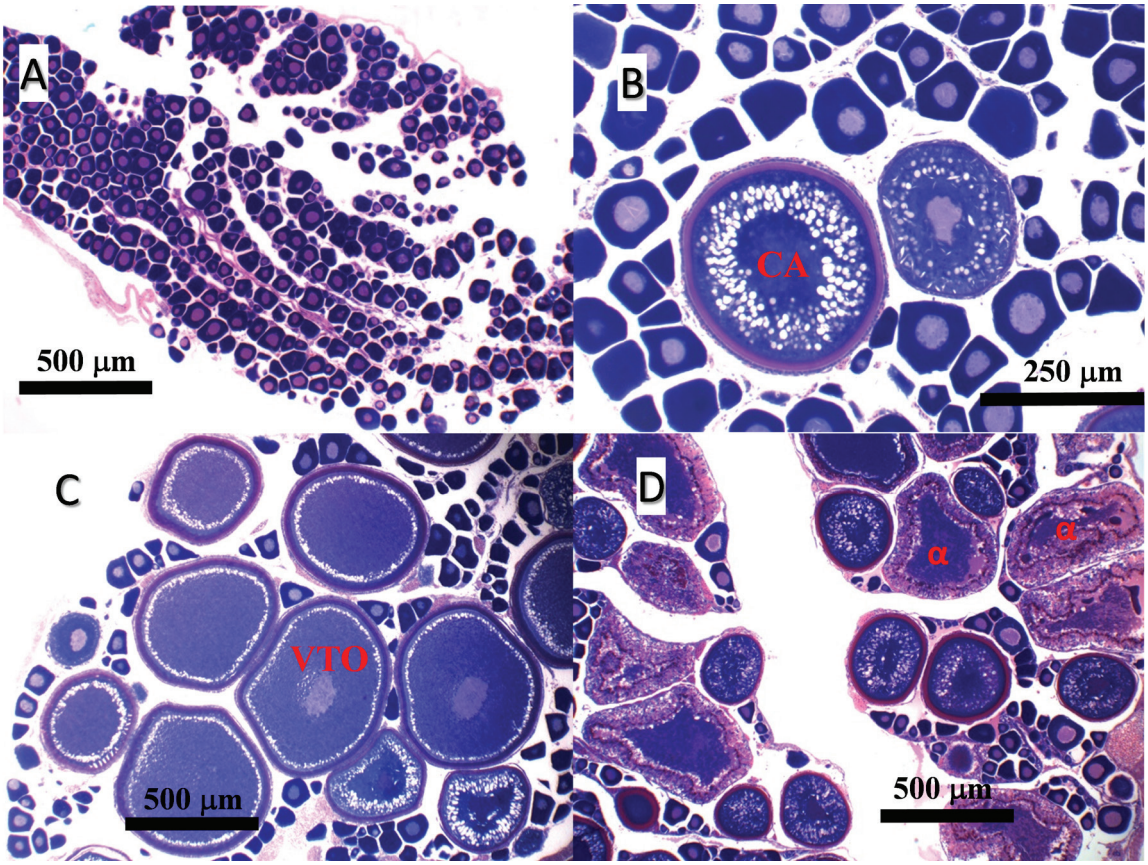

Fig. 3: Histological sections of ovaries. (A) Ovary of an immature fish with previtellogenic oocytes (September). (B) Ovary in the cortical alveoli stage (November). (C) Ovary in advanced vitellogenesis (November). (D) Ovary in atretic state 2 (June). CA: Oocyte in the yolk vesicle stage. VTO: vitellogenic oocyte. α: atretic follicle.

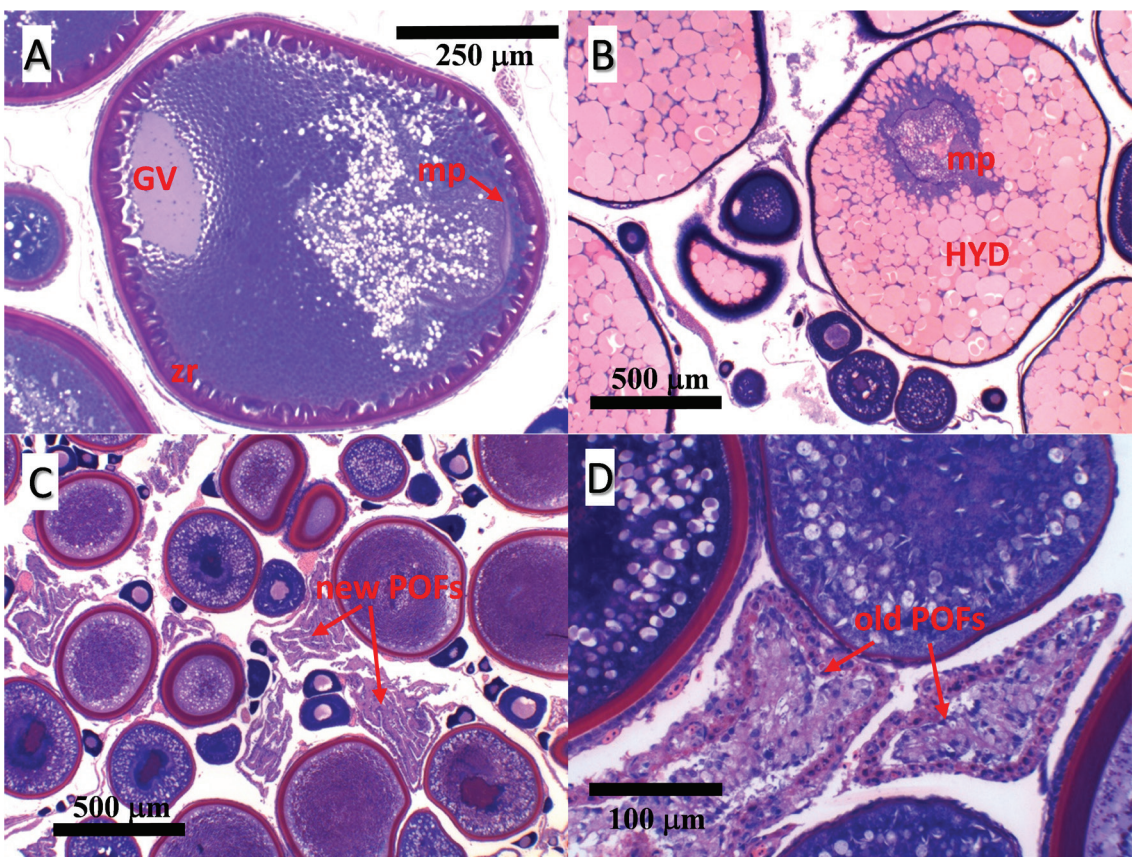

Fig. 4: Histological sections of ovaries. (A) Oocyte undergoing germinal vesicle migration. (B) Hydrated ovary. (C) Ovary with new postovulatory follicles (new POFs) (D) Ovary with postovulatory follicles in advanced degeneration (old POFs). GV: germinal vesicle. HYD: hydrated oocyte. zr: *zona radiata*. mp: ring-like structure (micropyle).

had apparently ceased with ovaries in the previtellogenic (PVO) stage or atretic states 2 and 3 (Table 2).

The main histological characteristics of growing oocytes in *E. golanii* were: (a) the absence of lipid droplets, (b) the division of *zona radiata* into two layers, inner and outer (also noted by Osman *et al.*, [2011]), with the inner *zona radiata* appearing highly convoluted during the germinal vesicle migration stage (Fig. 4A), and (c) the appearance of a ring-like structure during final maturation (Fig. 4A and 4B), most probably associated with the micropyle (Fig. 4A). Such a ring-like structure surrounding the micropyle has also been observed in scanning electron microscope preparations of *Etrumeus* eggs collected from the plankton off South Africa (Olivar & Fortuño, 1991).

Pattern of oocyte development

Figure 5 exemplifies the pattern of oocyte development, using the volume-based OSFDs, for a suite of 20 fish caught in April-May. The size hiatus between the advanced batch (AB) and smaller oocytes started to develop soon after the previous spawning event: Females with new POFs did not exhibit size gaps in OSFDs, whereas 18 out of the 19 examined females with old POFs had a fully developed hiatus separating the AB from the remaining, less developed oocytes. The separation of the AB from the subsequent batch (SB) occurred between 500 - 600 µm (e.g., Fig. 2). The hiatus became increasingly wide as the AB gained size at stages GVM and HYD (Fig. 5). In some advanced GVM ovaries and at the HYD stage, the formation of the SB started to become evident, by the appearance of two modes in the size frequency distributions of smaller oocytes (Fig. 5).

To study ovarian dynamics in more detail, we used the females with oocyte size measurements (n = 60) and calculated the proportion of oocytes in the AB (i.e. [number of oocytes in the AB]/[number of all oocytes >250 µm]). The enumeration of oocytes in the AB was carried out only in females with a fully developed hiatus in the respective OSFDs. Then, we calculated the proportion of oocytes >500 µm, not belonging to the completely separated AB (thereafter referred to as SB for simplicity) (i.e. [number of oocytes in the SB]/[number of all oocytes >250 µm]). Oocyte numbers were first raised to the whole ovary, based on subsample weights and gonad weight. The analysis showed (Fig. 6) that the mean fraction of oocytes in the AB was 23% in females with old POFs or GVM whereas the fraction of oocytes in the SB increased from 5% (old POFs) to 10% (GVM), reaching 23% at oocyte hydration (HYD). This implies that the number of oocytes required to form the next batch increases fast at final maturation and, at hydration, the next batch has already been fully recruited. In females with new POFs, the mean fraction of oocytes >500µm was 26% (not shown).

Interestingly, the mean maximum diameter of oocytes in the SB did not change (~630 µm) from the time of separation of the AB (in females with old POFs) to oocyte hydration (Fig. 6). Secondary growth of oocytes in the SB is therefore practically arrested until the release of the AB. Mean maximum oocyte diameter in females with new POFs was 643 µm.

Ovarian and somatic condition

Significant terms of the general linear models for ovarian and somatic condition are shown in Table 3. All models had a good fit in terms of residuals (normally distributed, homoscedastic) and explained a large amount of

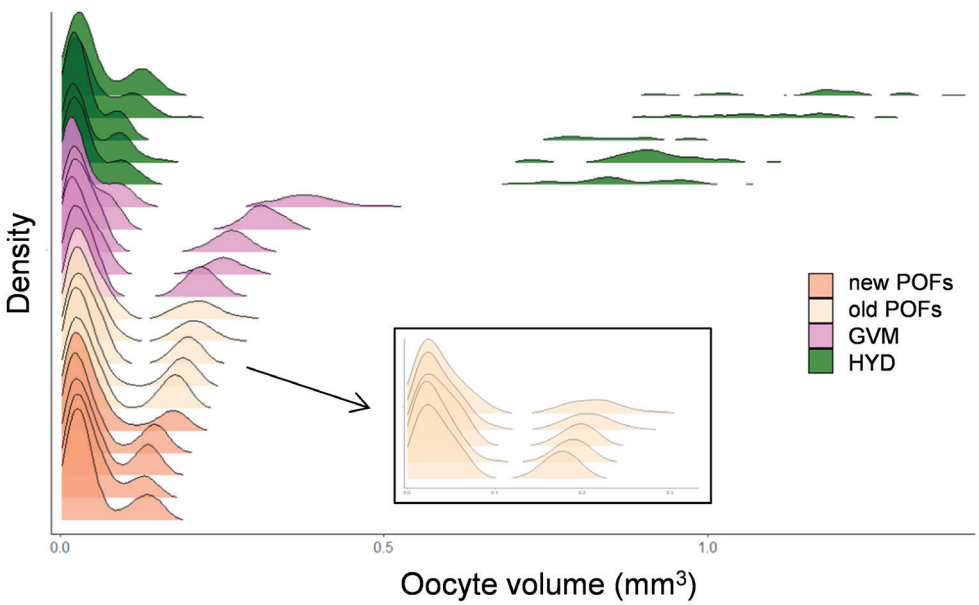

Fig. 5: Spawning capable females. Fitted oocyte size densities for selected females with markers of previous (POFs) and imminent spawning (GVM or HYD). They are presented in ascending order of maximum oocyte volume (nested inside ovarian category). Oocyte-size densities of females with old POFs are also plotted separately to highlight the already developed size gap between the advanced batch and the remaining, less developed oocytes.

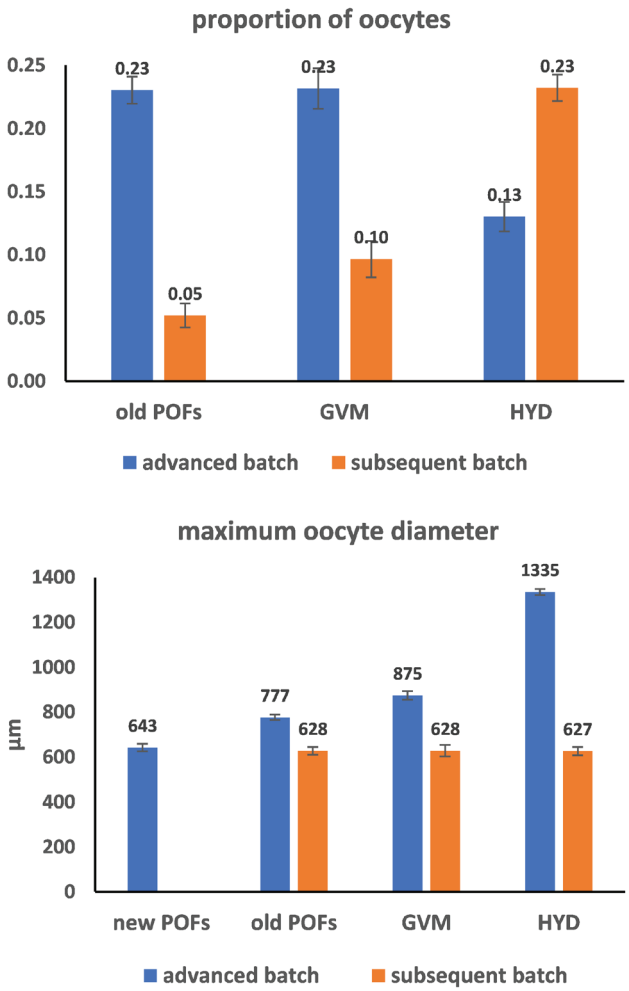

Fig. 6: Numerical fraction (i.e. number of oocytes -on- total number of oocytes >250µm) and maximum oocyte diameter of the advanced batch (AB) and the subsequent batch (SB). The SB is considered to include oocytes >500 µm, not contained within the AB. The number of oocytes in the AB was counted only in females with a fully developed size gap in the respective OSFDs. Error bars are standard errors and data labels are average values.

variation (93% - 99%). The term MONTH was highly significant in all models. The effect of YEAR was not significant except for the female somatic condition model, in which it accounted for a high percentage of the modelled variability (Table 3). This significant YEAR effect was associated with a trend of increasing average condition of females from 2016 to 2019 (not shown). The term MONTH × YEAR entered in three of the four models, accounting for small year-to-year variations in monthly condition, partly attributable to differences in sample size (Table 3).

Monthly least square means (average monthly condition) of females and males are shown in Figure 7. Gonadal condition started to increase in November/December and exhibited the highest mean values from January to May. In June, average gonadal condition decreased and then dropped substantially in July/September. The hydrographic/biogeochemical model simulation (Fig. 8) showed that the start of gonadal maturation in late autumn is associated with the period of decreasing SST and increasing Chl-α (i.e., start of the mixing period). The period of June-October is characterized by the highest SSTs (>23°C) and decreasing mesozooplankton availability. The mean mesozooplankton concentration starts to increase in January, peaks in March-April, i.e. approximately one month after the Chl-α bloom, and then starts to decrease.

Somatic condition showed an overall increasing trend from winter to July, which appeared to be followed by an opposite, decreasing trend, especially in females. The somatic condition of females reached the lowest levels in December - January, i.e. at the beginning of the annual spawning period. In both males and females, a peak in somatic condition occurred in July, i.e. immediately after the end of the annual spawning period (Fig. 7).

Table 3. Gonadal and somatic condition of female and male *Etrumeus golanii*. Results of the final general linear models with gonad weight (GW) and gonad-free weight (GFW) as dependent variables. MONTH: month of sampling. YEAR: year of sampling. X: GFW or TL for gonadal and somatic condition respectively. Least-square means for the term MONTH are shown in Figure 7.

	females				**males**			
	gonadal condition log(GW)		**somatic condition log(GFW)**		**gonadal condition log(GW)**		**somatic condition log(GFW)**	
Effect	**F**	**η_p^2**	**F**	**η_p^2**	**F**	**η_p^2**	**F**	**η_p^2**
MONTH	12.08***	0.264	24.08***	0.098	211.81***	0.879	3.25**	0.093
YEAR	a		11.252***	0.410	a		A	
log(X)	165.81***	0.354	12204.69***	0.975	265.60***	0.503	1793.52***	0.877
MONTH×YEAR	9.93***	0.164	5.91**	0.054	a		6.67***	0.117
MONTH×log(X)	5.47***	0.140	a		a		3.21**	0.092
YEAR×log(X)	a		a		2.97*	0.033	A	
adj.-r^2	0.934		0.994		0.946		0.995	

η_p^2: Partial-eta squared (proportion of the effect + error variance that is attributable to the effect); a: effect that was left out by the stepwise procedure; *: p<0.05, **: p<0.01, ***: p<0.001.

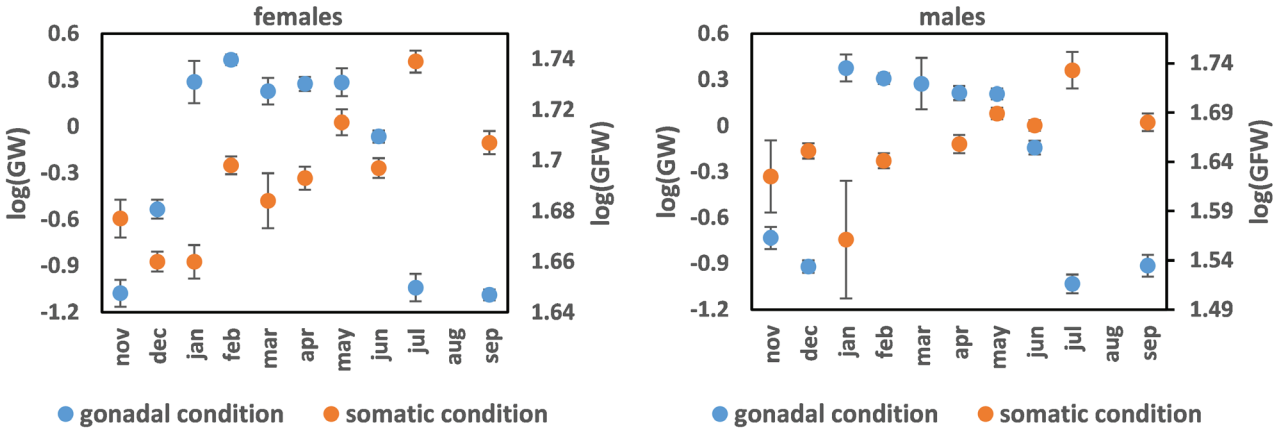

Fig. 7: Monthly least-square means of female and male gonadal and somatic condition. Error bars are standard errors. GW: gonad weight (g). GFW: gonad-free weight (g).

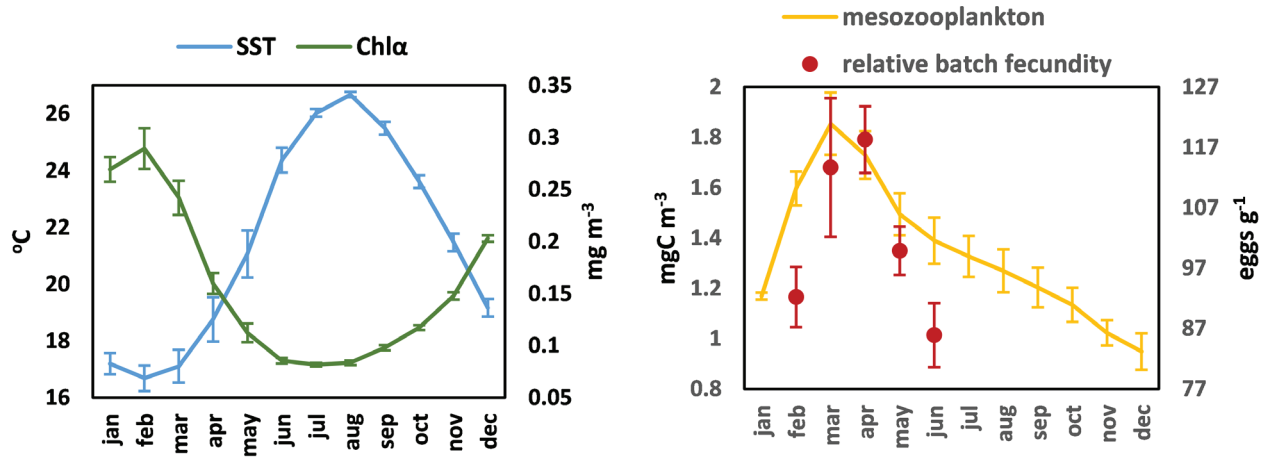

Fig. 8: Model-simulated sea-surface temperature (SST) and chlorophyll α (Chlα) (left panel) and mesozooplankton concentration (0-100 m) (right panel) in the period 2016-2019. Mean monthly relative batch fecundity of *Etrumeus golanii* is also plotted (right panel). Error bars are standard errors for fecundity and standard deviations for modelled variables.

Batch fecundity

Batch fecundity was measured in all females at final maturation (GVM and HYD) and 18 females with old POFs caught in March-May (see above), with a fully developed size gap between the AB and the remaining oocytes (overall n = 71). The comparison of batch fecundity -on- gonad-free weight relationships between females with old POFs and females in final maturation, for the period of March-May (n = 41), revealed homogeneous slopes ($F = 0.22$, $p = 0.640$) and intercepts ($F = 1.52$, $p = 0.226$) (ANCOVA models).

The relationships between batch fecundity (BF) and gonad-free weight (GFW) or total length (TL) were better described by power (log - log) functions (e.g., Fig. 9). The overall batch fecundity relationships (pooled sample) were:

$\log(BF) = 1.111 \times \log(GFW) + 1.788$, $r^2 = 0.880$, and,
$\log(BF) = 3.497 \times \log(TL) - 4.229$, $r^2 = 0.873$.

Analysis of covariance (ANCOVA) models showed that the intercepts of the BF -on- GFW relationship differed significantly between months (slopes: $F = 0.93$, $p = 0.45$; intercepts: $F = 4.72$, $p = 0.002$). Relative batch fecundity (RF = BF / GFW) ranged from 56 to 157 eggs g^{-1} and also differed significantly (ANOVA, $F = 5.46$, $p < 0.001$) between the sampling months (Table 4). These monthly changes in BF and RF appeared to follow closely the mean simulated mesozooplankton concentration (Fig. 8).

Table 4. Mean relative batch fecundity (RF = BF / GFW). N = number of females. a < b: homogeneous groups (Bonferroni tests).

Month	N	RF (eggs g^{-1})
feb	16	92^{a}
mar	3	$114^{a,b}$
apr	13	118^{b}
may	25	$100^{a,b}$
jun	14	86^{a}
Total	71	99

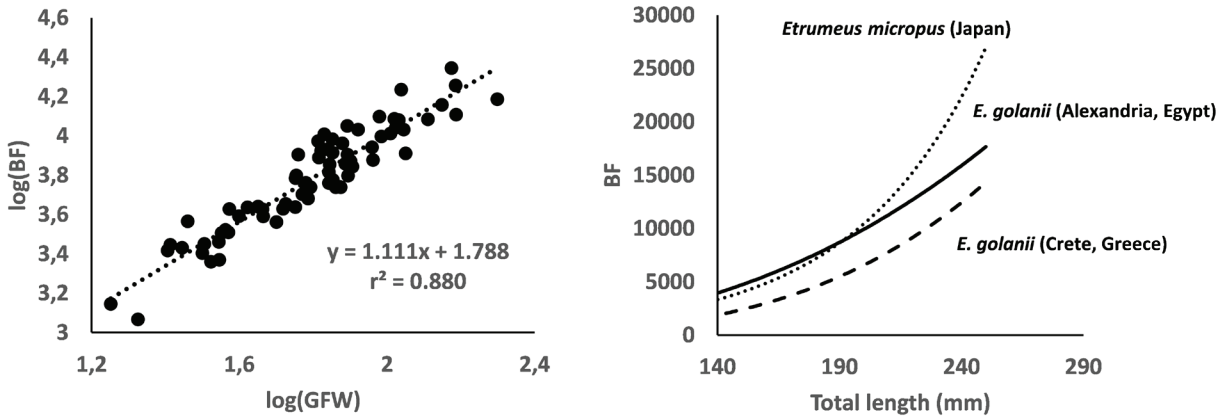

Fig. 9: Batch fecundity (BF) -on- size relationships. Left: The BF -on- Gonad free weight (GFW) for *Etrumeus golanii* off Crete. Right: The BF -on- Total length relationships for different *Etrumeus* stocks/species (*E. golanii*: present study, Osman *et al.*, [2011]. *E. micropus*: Nyuji & Takasuka, [2017]).

Discussion

There are currently eight recognized species of genus *Etrumeus* Bleeker 1853, distributed globally in shelf waters between 40°N and 40°S (DiBattista *et al.,* 2012; 2014; Randal & DiBattista, 2012; Whitehead, 1985). They were formerly known as a single species, *Etrumeus teres* (DeKay, 1842). Although information on their reproductive biology is scarce, existing studies suggest that they present many similarities, particularly with regard to the timing of the main spawning period (winter-spring), fecundity type (indeterminate), and egg size (larger eggs compared to other clupeoids with pelagic eggs).

Spawning period

In this study, *E. golanii* is shown to have a prolonged breeding season with the main spawning activity extending from January to May. During these months, the incidence of atresia was nil and all females examined histologically had markers of recent (POFs) and/or imminent spawning (oocytes in final maturation). Gonadal condition started to increase in November/December and remained high until early summer (June). Most females in November/December were at the CA stage (start of secondary growth phase), with even occasional incidence of vitellogenic individuals. The first appearance of postspawning females (with mass follicular atresia) was observed in June. In July, gonadal condition dropped substantially and all females examined were in postspawning (atretic) or resting condition. In the Egyptian Mediterranean Sea, Osman *et al.* (2011) also found that this species exhibited a prolonged spawning season, starting in December and ending in early summer. In the latter study, spent (post-spawning) fish were only recorded in summer (June, July and August). Similar results have been reported by El-Sayed (1996, cited in Osman *et al.*, [2011]) for *E. golanii* in the Gulf of Suez (Red Sea).

In general, it appears that the main spawning period of *Etrumeus* species is between winter and late spring. Spawning of the east African round herring *Etrumeus wongratanai* DiBattista, Bowen & Randall 2012 takes place from the onset of austral winter to early summer (Vorsatz *et al.*, 2019). The peak spawning period of the Whitehead's (West African) round herring *Etrumeus whiteheadi* Wongratana 1983 occurs from August to October (austral winter/spring) and spawning takes place over a prolonged season (Roel & Melo, 1990). Off southern Japan (Plaza *et al.*, 2007), mature and recently spawned females *Etrumeus micropus* (Temminck & Schlegel 1846) occurred all year round, except for summer. Spawning stopped in July and August and peaked in winter and spring. In the Gulf of Mexico, the main spawning period of *Etrumeus sadina* (Mitchill 1814) is between winter and late spring (Fahay, 1983; Shaw & Drullinger, 1990).

Pattern of oocyte development

This study confirms that *E. golanii* is a multiple spawning fish with indeterminate annual fecundity. This appears to be true for all species of the genus *Etrumeus* that have been studied so far using ovarian histology and analysis of OSFDs (i.e. African & West Pacific species: Roel & Melo, 1990; Plaza *et al.*, 2007; Osman *et al.*, 2011; Nyuji & Takasuka, 2017). Apart from the protracted spawning season (see above), the co-occurrence of all stages of oocyte development in the ovaries of actively spawning fish, the incidence of markers of either recent or imminent spawning, all along the protracted spawning period, and the massive atresia observed towards the end of the spawning season, are all strong indications of indeterminate annual fecundity (Murua & Saborido-Rey, 2003; Armstrong & Witthames, 2012).

The detailed analysis of oocyte sizes carried out for this study shows that, during the final maturation of the advanced batch (AB), a new batch (SB) starts to recruit rapidly to sizes >500 μm and, after the release of the AB, grows quickly in size, separates from the smaller oocytes and becomes the new AB. Eighteen (18) out of the 19 examined females with old POFs (95%), had an already

developed size gap between the AB (consisting of the larger VTO oocytes) and the remaining, smaller oocytes. The growth of these smaller oocytes (SB) to sizes >500 μm appeared to be very slow and practically stopped until the hydration of the AB. Maximum diameters of oocytes in the SB were steadily smaller than 630 μm up to the release of the AB. These findings are consistent with those reported for *E. micropus* off southern Japan (Plaza *et al.*, 2007; Nyuji & Takasuka, 2017). Plaza *et al.* (2007) observed that while oocytes in the AB were growing to maturation, the development and growth of the SB, "mainly composed of CA stage oocytes", stopped. When hydration started in the AB, the CA oocytes of the SB entered into true vitellogenesis, resulting in bimodal size frequency distributions of smaller (non-hydrated) oocytes. Nyuji & Takasuka (2017) found that the maximum diameter of oocytes in the SB was 449.1 ± 29.8 μm at the early GVM stage and 494.3 ± 31.9 μm at the HYD stage. These values are lower than those found in this study (~630 μm) and can be attributed to a temperature effect on oocyte growth rate (Yoneda *et al.*, 2014; Somarakis *et al.*, 2019). Female *E. golanii* examined here were collected in spring (mainly April - May) at a mean SST of about 20° C (see Fig. 8) whereas Nyuji & Takasuka (2017) analyzed fish collected in February, at water temperatures of about 17° C.

Somatic condition

Monthly changes in somatic condition of *E. golanii* were low, albeit significant, showing a prominent peak in July, i.e. immediately after the end of the annual spawning period. A similar peak has been observed for the same species in the Egyptian Mediterranean Sea (Farrag *et al.*, 2014). It may be attributed to the cessation of spawning activity, combined with an increased consumption of high energy prey such as fish larvae, especially anchovy *Engraulis encrasicolus* and round sardinella *Sardinella aurita* larvae, which are particularly abundant in the eastern Mediterranean during July (Tsoukali *et al.*, 2019; and references therein). Indeed, Osman *et al.* (2013) observed that the diet of *E. golanii* included high quantities of fish larvae in summer, which these authors attributed to their increased abundance at that time of the year. High consumption of fish larvae in summer has also been reported for *E. wongratanai* off the east coast of South Africa (Vorsatz *et al.*, 2019).

The seasonal patterns in somatic condition inferred from this study should be treated with caution due to the opportunistic nature of sample collection. In the GLM for females, the effect of YEAR accounted for a high amount of variability, implying high interannual differences (see results). In plots of monthly averages, an overall increasing trend was noted from winter to July, which appeared to be followed by an opposite, decreasing trend, especially in females. Similarly, in *E. wongratanai* off South Africa, the lowest somatic condition was observed between April and August (austral autumn to winter) and the condition increased between September and January (spring to summer) (Vorsatz *et al.*, 2019). In the latter study, high interannual variability was also observed, occasionally masking the usual seasonal pattern. Off southern Japan, the somatic condition of *E. micropus* peaked from summer to mid-autumn (Plaza *et al.*, 2007), which contradicts our observations, namely, that somatic condition of *E. golanii* deteriorates from summer to autumn.

The phase of increasing somatic condition inferred from this study matches the timing of the breeding season, which starts during the winter mixing period and subsequently includes the period of increased mesozooplankton concentration and increasing SST (Fig. 8). This suggests that *E. golanii* exploits the increased food resources associated with the annual plankton cycle to acquire energy for both the soma and egg production. It therefore appears to be closer to the income breeding mode (McBride *et al.*, 2015; Somarakis *et al.*, 2019).

The deterioration of body condition observed from summer to autumn can be attributed to the combined effect of low prey availability and high temperature. High subsurface temperatures encountered in the eastern Mediterranean during the stratified period can often be stressful leading to reduced plankton consumption compared to winter (Nikolioudakis *et al.*, 2011; 2014). Furthermore, high temperatures increase maintenance costs substantially (respiration, etc) in a period when prey availability for small pelagic fish is, in any case, low (Gkanasos *et al.*, 2019). In the latter study, field data and bioenergetic modelling showed that, in the Aegean Sea, both anchovy (*Engraulis encrasicolus*) and sardine (*Sardina pilchardus*) increase their energy reserves from winter to early summer, but, from mid-summer onwards, their somatic condition declines sharply, which agrees with the present observations for *E. golanii*.

Batch fecundity

The generic hydrodynamic/biogeochemical ecosystem model implemented in this study has been shown (see also Supplementary material) to reasonably reproduce the seasonal variability of the main biogeochemical and planktonic features of the Mediterranean ecosystem, as influenced by the seasonal variability of the thermocline and vertical mixing in the water column (Kalaroni *et al.*, 2020a,b). According to the model simulation (Fig. S2, Fig. 8), the Chl-α bloom occurs in February/March and is followed by a mesozooplankton maximum, after approximately one month. This is in agreement with available time series of *in situ* data showing that the seasonal mesozooplankton and copepod peak in the Mediterranean Sea succeeds the Chl-α maximum with a time lag of approximately 1-2 months (Berline *et al.*, 2012; Fullgrabe *et al.*, 2020). We found significant monthly changes in average batch fecundity of *E. golanii* off the coasts of Crete, which appeared to follow closely the simulated mean mesozooplankton concentration, presumably with a time lag of about one month (Fig. 8). This observation implies a trophic influence on fecundity variations of *E. golanii*. Batch fecundity is highly variable within a small pelagic species and may vary during

the spawning season (Ganias *et al.*, 2014b). In general, it is higher during peak spawning and lower near the start and end of the reproductive period (e.g., in sprat, Alheit [1989]; Japanese anchovy, Tsuruta & Hirose [1989]; Bay anchovy, Luo & Musick [1991]; European sardine, Zwolinski *et al.*, [2001]). In many species, batch fecundity appears to be sensitive to food availability. For example, Somarakis (2005) found significantly higher egg production, batch fecundity and spawning frequency for anchovy *E. encrasicolus* in the North Aegean Sea in June 1993, compared to June 1995, which was attributed to significantly higher mesozooplankton concentration in 1993. Milton *et al.* (1995) found that batch fecundity in several tropical clupeoids was positively correlated with zooplankton density.

Finally, average batch fecundity estimates for *E. golanii* off the coasts of Crete were lower than those along the Egyptian Mediterranean coasts (Osman *et al.*, 2011) or estimates for *E. micropus* off southern Japan (Nyuji & Takasuka, 2017) (Fig. 9). This difference can also be explained in terms of food availability. In the Egyptian Mediterranean Sea, large increases in fertilizer application and sewage discharge in Egypt since the mid-1980s have resulted in rapid increases in nutrient loading and a dramatic recovery of the highly productive coastal Mediterranean fishery off the Nile River delta, which had collapsed after the completion of the Aswan High Dam in 1965 (Oczkowski *et al.*, 2009).

Compared to other clupeoid fishes with pelagic eggs, species of the genus *Etrumeus* appear to have lower relative fecundities and larger egg size. For example, the diameters of hydrated oocytes in the Mediterranean sardine *S. pilchardus* ranged between 750 and 1000 μm and relative batch fecundity was >300 eggs g^{-1} during the peak of the spawning season (Ganias *et al.*, 2004). In contrast, mean oocyte diameters of *E. golanii* hydrated oocytes ranged between 1181 and 1325 μm (see also Plaza *et al.* [2007]) and average RF was about 100 eggs g^{-1} during peak spawning period.

E. golanii is the only Lessepsian small pelagic fish that expanded so rapidly from the eastern to the western Mediterranean and established local populations in many areas of the oligotrophic southern Mediterranean Sea. It can therefore be considered as a successful invader. This seems to be due, at least in part, to its reproductive characteristics, namely, the prolonged, winter/spring spawning period that takes advantage of the seasonal cycle of plankton production, as influenced by the seasonal variability of the thermocline and vertical mixing in the water column, and its large egg size that increases the chances of survival for developing embryos and larvae (Houde, 2009). The pattern of oocyte development demonstrated for *Etrumeus* (in which the secondary growth of the SB is practically arrested until spawning of the AB) and the low relative batch fecundities can be considered as adaptations allowing for the production of successive batches of large pelagic eggs over a protracted spawning season (Plaza *et al.*, 2007).

Acknowledgements

We would like to thank all the staff of the Institute of Marine Biological Resources and Inland Waters in Crete who participated in the onboard samplings and laboratory analysis of round herring samples. Special thanks are due to Giannis Kosoglou, Giorgos Lazarakis and Kostas Skarvelis.

References

Alheit, J., 1989. Comparative spawning biology of anchovies, sardines, and sprats. *Rapports et procès-verbaux des réunions / Conseil permanent international pour l'exploration de la mer*, 191, 7-14.

Armstrong, M.J., Witthames, P.R., 2012. Developments in understanding of fecundity of fish stocks in relation to egg production methods for estimating spawning stock biomass. *Fisheries Research*, 117-118, 35-47.

Bennett, H.S., Wyrick, A.D., Lee, S.W., McNeil, J.H., 1976. Science and art in preparing tissues embedded in plastic for light microscopy, with special reference to glycol methacrylate, glass knives, and simple stains. *Stain Technology*, 51 (2), 71-94.

Berline, L., Siokou-Frangou, I., Marasovic, I., Vidjak, O., Fernandez de Puelles, M. *et al.*, 2012. Intercomparison of six Mediterranean zooplankton time series. *Progress in Oceanography*, 97-100, 76-91.

Brown-Peterson, N.J., Wyanski, D.M., Saborido-Rey, F., Macewicz, B.J., Lowerre-Barbieri, S.K., 2011. A standardized terminology for describing reproductive development in fishes. *Marine and Coastal Fisheries*, 3 (1), 52-70.

Çiftçi, S.E., Bardakci, F., 2021. A Lessepsian invader round herring (*Etrumeus golanii*) with high genetic diversity without bottlenecking in the northeastern Mediterranean Sea. *Turkish Journal of Zoology*, 45, 102-107.

DiBattista, J., Randall, J., Bowen, B., 2012. Review of the round herrings of the genus *Etrumeus* (Clupeidae: Dussumieriinae) of Africa, with descriptions of two new species. *Cybium*, 36 (3), 447-460.

DiBattista, J.D., Randall, J.E., Newman, S.J., Bowen, B.W., 2014. Round herring (genus *Etrumeus*) contain distinct evolutionary lineages coincident with a biogeographic barrier along Australia's southern temperate coastline. *Marine Biology*, 161, 2465-2477.

Fahay, M.P., 1983. *Guide to the early stages of marine fishes occurring in the western North Atlantic Ocean, Cape Hatteras to the southern Scotian Shelf*. Journal of the Northwest Atlantic Fisheries Science, Vol. 4, Northwest Atlantic Fisheries Organization, Dartmouth, Canada, 423 pp.

Farrag, M.M., Osman, A.G., Akel, E.S.H.K., Moustafa, M.A., 2014. Catch and effort of night purse seine with emphasize to age and growth of lessepsian *Etrumeus teres* (Dekay, 1842), Mediterranean Sea, Egypt. *The Egyptian Journal of Aquatic Research*, 40, 181- 190.

Follesa, M.C., Carbonara, P. (Eds)., 2019. *Atlas of the maturity stages of Mediterranean fishery resources.* Studies and Reviews n. 99, FAO, Rome, 268 pp.

Fullgrabe, L., Grosjean, P., Gobert, S., Lejeune, P., Leduc, M.

et al., 2020. Zooplankton dynamics in a changing environment: A 13-year survey in the northwestern Mediterranean Sea. *Marine Environmental Research*, 159, 104962.

Galil, B.S., Danovaro, R., Rothman, S.B.S., Gevili, R., Goren, M., 2019. Invasive biota in the deep-sea Mediterranean: an emerging issue in marine conservation and management. *Biological Invasions*, 21, 281-288.

Galil, B.S., Mienis, H.K., Hoffman, R., Goren, M., 2021. Non-indigenous species along the Israeli Mediterranean coast: tally, policy, outlook. *Hydrobiologia*, 848, 2011-2029.

Ganias, K., Somarakis, S., Machias, A., Theodorou, A., 2004. Pattern of oocyte development and batch fecundity in the Mediterranean sardine. *Fisheries Research*, 67 (1), 13-23.

Ganias, K., Somarakis, S., Koutsikopoulos, C., Machias, A., 2007. Factors affecting the spawning period of sardine in two highly oligotrophic Seas. *Marine Biology*, 151, 1559-1569.

Ganias, K., Murua, H., Claramunt, G., Dominguez-Petit, R., Gonçalves, P. *et al.*, 2014a. Chapter 4: Egg production. 109 pp. In: *Handbook of applied fisheries reproductive biology for stock assessment and management*. Domínguez-Petit, R., Murua, H., Saborido-Rey, F., Trippel. E. (Eds). Digital CSIC, Vigo, Spain, https://digital.csic.es/handle/10261/87768.

Ganias, K., Somarakis, S., Nunes, C., 2014b. Reproductive potential. pp. 79-121. In: *Biology and Ecology of sardines and anchovies*. Ganias, K. (Ed). CRC Press, Taylor & Francis Group, Boca Raton.

Geladakis, G., Nikolioudakis, N., Koumoundouros, G., Somarakis, S., 2018. Morphometric discrimination of pelagic fish stocks challenged by variation in body condition. *ICES Journal of Marine Science*, 75 (2), 711-718.

Giannakaki, A., Skarvelis, K., Peristeraki, P., Somarakis, S., 2018. Preliminary results on biological parameters of round herring *Etrumeus golanii* in Cretan waters. p. 35. In: *12th Panhellenic Symposium of Oceanography & Fisheries*, *Corfu, 30 May – 3 June 2018*. HCMR, Athens.

Gkanasos, A., Somarakis, S., Tsiaras, K., Kleftogiannis, D., Giannoulaki, M. *et al.*, 2019. Development, application and evaluation of a 1-D full life cycle anchovy and sardine model for the North Aegean Sea (Eastern Mediterranean). *PLoS ONE* 14 (8), e0219671.

Golani, D., 1998. Impact of Red Sea fish migrants through the Suez Canal on the aquatic environment of the Eastern Mediterranean. In: *Transformations of Middle Eastern Natural Environments: Legacies and Lessons*. Albert, J., Bernhardsson M., Kenna R. (Eds). Yale University Conference. *Yale University School of Forestry and Environmental Studies Bulletin*, 103, 375-387.

Houde, E.D., 2009. Recruitment variability. p. 91−171. In: *Fish reproductive biology: implications for assessment and management*. Jakobsen, T., Fogarty, M.J., Megrey, B.A., Moksness, E. (Eds). Wiley-Blackwell, Oxford.

Hunter, J.R., Macewicz, B.J., 1985a. Measurement of spawning frequency in multiple spawning fishes. pp. 79-94. In: *An Egg Production Method for Estimating Spawning Biomass of Pelagic Fish: Application to the Northern Anchovy, Engraulis mordax*. Lasker, R. (Ed). NOAA Technical Report NMFS 36.

Hunter, J.R., Macewicz, B.J., 1985b. Rates of atresia in the ovary of captive and wild northern anchovy, *Engraulis mordax*. *Fishery Bulletin*. 83 (2), 119-136.

Hunter, J.R., Lo, N.C.H., Leong, R.J.H., 1985. Batch fecundity in multiple spawning fishes. pp. 67-78. In: *An Egg Production Method for Estimating Spawning Biomass of Pelagic Fish: Application to the Northern Anchovy,* Engraulis mordax. Lasker, R. (Ed). NOAA Technical Report NMFS 36.

Kalaroni, S., Tsiaras, K., Petihakis, G., Economou-Amilli, A., Triantafyllou, G., 2020a. Modelling the Mediterranean pelagic ecosystem using the POSEIDON ecological model. Part I: Nutrients and chlorophyll-a dynamics. *Deep Sea Research Part II: Topical Studies in Oceanography*, 171, 104647.

Kalaroni, S., Tsiaras, K., Petihakis, G., Economou-Amilli, A., Triantafyllou, G., 2020b. Modelling the mediterranean pelagic ecosystem using the POSEIDON ecological model. Part II: Biological dynamics. *Deep Sea Research Part II: Topical Studies in Oceanography*, 171, 104711.

Kasapidis, P., Peristeraki, P., Tserpes, G., Magoulas, A., 2007. A new record of the Lessepsian invasive fish *Etrumeus teres* (Osteichthyes: Clupeidae) in the Mediterranean Sea (Aegean, Greece). *Aquatic Invasions*, 2 (2), 152-154.

Katsanevakis, S., Wallentinus, I., Zenetos, A., Leppäkoski, E., Çinar, M.E. *et al.*, 2014. Impacts of invasive alien marine species on ecosystem services and biodiversity: a pan-European review. *Aquatic Invasions*, 9 (4), 391-423.

Luo, J.G., Musick, J.A., 1991. Reproductive biology of the bay anchovy in Chesapeake Bay. *Transactions of the American Fisheries Society*, 120 (6), 701-710.

McBride, R.S., Somarakis, S., Fitzhugh, G.R., Albert, A., Yaragina, N.A. *et al.*, 2015. Energy acquisition and allocation to egg production in relation to fish reproductive strategies. *Fish and Fisheries*, 16 (1), 23-57.

Milton, D., Blaber, S., Rawlinson, N., 1995. Fecundity and egg production of four species of short-lived clupeoid from Solomon Islands, tropical South Pacific. *ICES Journal of Marine Science*, 52 (1), 111-125.

Murua, H., Saborido-Rey, F., 2003. Female reproductive strategies of commercially important fish species in the North Atlantic. *Journal of the Northwest Atlantic Fisheries Science*, 33, 23-32.

Nikolioudakis, N., Palomera, I., Machias, A., Somarakis, S., 2011. Diel feeding intensity and daily ration of the sardine *Sardina pilchardus*. *Marine Ecology Progress Series*, 437, 215-228.

Nikolioudakis, N., Isari, S., Somarakis, S., 2014. Trophodynamics of anchovy in a non-upwelling system: Direct comparison with sardine. *Marine Ecology Progress Series*, 500, 215-229.

Nyuji, M., Takasuka, A., 2017. Spawning cycle and fecundity of a multiple spawner round herring *Etrumeus teres* off southern Japan: Oocyte growth and maturation analysis. *Journal of Sea Research*, 122, 11-18.

Oczkowski, A.J., Nixon, S.W., Granger, S.L., El-Sayed, A.-F.M., McKinney, R.A., 2009. Anthropogenic enhancement of Egypt's Mediterranean fishery. *Proceedings of the National Academy of Sciences of the United States of America*, 106 (5), 1364-1367.

Olivar, M.P., Fortuño, J.M., 1991. Guide to ichthyoplankton of

the Southeast Atlantic (Benguela Current Region). *Scientia Marina*, 55 (1), 1-383.

Osman, A.G., Akel, E.S.H.K., Farrag, M., Moustafa, M.A., 2011. Reproductive biology of round herring *Etrumeus teres* (Dekay, 1842) from the Egyptian Mediterranean water at Alexandria. *ISRN Zoology*, 2011, 1-12.

Osman, A.G., Farrag, M., Akel, E.S.H.K., Moustafa, M.A., 2013. Feeding behavior of lessepsian fish *Etrumeus teres* (Dekay, 1842) from the Mediterranean Waters, Egypt. *The Egyptian Journal of Aquatic Research*, 39 (4), 275-282.

Otero, M., Cebrian, E., Francour, P., Galil, B., Savini, D., 2013. *Monitoring Marine Invasive Species in Mediterranean Marine Protected Areas (MPAs): A Strategy and Practical Guide for Managers*. MedPAN North project. IUCN, Malaga, Spain. 136 pp.

Plaza, G., Sakaji, H., Honda, H., Hirota, Y., Nashida, K., 2007. Spawning pattern and type of fecundity in relation to ovarian allometry in the round herring *Etrumeus teres*. Marine Biology, 152 (5), 1051-1064.

Randall, J.E., DiBattista, J.D., 2012. *Etrumeus makiawa*, a New Species of Round Herring (Clupeidae: Dussumierinae) from the Hawaiian Islands. *Pacific Science* 66 (1), 97-110.

Roel, B.A., Melo, Y.C., 1990. Reproductive biology of round herring *Etrumeus whiteheadi*. *South African Journal of Marine Science*, 9 (1), 177-187.

Schismenou, E., Somarakis, S., Thorsen, A., Kjesbu, O.S., 2012. Dynamics of *de novo* vitellogenesis in fish with indeterminate fecundity: an application of oocyte packing density theory to European anchovy, *Engraulis encrasicolus*. *Marine Biology*, 159, 757-768.

Shaw, R.F., Drullinger, D.L., 1990. *Early life-history profiles, seasonal abundance and distribution of four species of clupeid larvae from the Northern Gulf of Mexico, 1982 and 1983.* NOAA Technical Report NMFS 88, Springfield, NOAA. 60 pp.

Somarakis, S., 2005. Marked inter-annual differences in reproductive parameters and daily egg production of anchovy in the northern Aegean Sea. *Belgian Journal of Zoology*, 135 (2), 247-252.

Somarakis, S., Schismenou, E., Siapatis, A., Giannoulaki, M., Kallianiotis, A. *et al.*, 2012. High variability in the Daily Egg Production Method parameters of an eastern Mediterranean anchovy stock: Influence of environmental factors, fish condition and population density. *Fisheries Research*, 117-118, 12-21.

Somarakis, S., Tsoukali, S., Giannoulaki, M., Schismenou, E., Nikolioudakis, N., 2019. Spawning stock, egg production and larval survival in relation to small pelagic fish recruitment. *Marine Ecology Progress Series*, 617-618, 113-136.

Tamsouri, M.N., Benchoucha, S., Idhalla, M., El Aamri, F., 2019. *Etrumeus golanii* (Actinopterygii: Clupeiformes: Dussumieriidae) a new Lessepsian migrant recorded in Morocco, Alboran Sea (south-west Mediterranean). *Acta Ichthyologica et Piscatoria*, 49 (1), 43-47.

Thorsen, A., Kjesbu, O.S., 2001. A rapid method for estimation of oocyte size and potential fecundity in Atlantic cod using a computer-aided particle analysis system. *Journal of Sea Research*, 46 (3-4), 295-308.

Tsoukali, S., Giannoulaki, M., Siapatis, A., Schismenou, E., Somarakis, S., 2019. Using spatial indicators to investigate fish spawning strategies from ichthyoplankton surveys: A case study on co-occurring pelagic species from the North-East Aegean Sea. *Mediterranean Marine Science*, 20 (1), 106-119.

Tsuruta, Y., Hirose, K., 1989. Internal regulation of reproduction in the Japanese anchovy (*Engraulis japonica*) as related to population fluctuation. *Canadian Special Publication of Fisheries Aquatic Science*, 108, 111-119.

Vorsatz, L.D., van der Lingen, C.D., Gibbons, M.J., 2019. Observations on the biology and seasonal variation in feeding of the east coast round herring *Etrumeus wongratanai* (Clupeiformes), off Scottburgh, KwaZulu-Natal, South Africa. *Journal of Fish Biology*, 94 (3), 498-511.

Whitehead, P.J.P., 1985. *FAO species catalogue, Vol. 7. Clupeoid fishes of the world (suborder Clupeoidei). Part l — Chirocentridae, Clupeidae and Pristigasteridae*. FAO Fisheries synopsis 125, FAO, Rome. 303 pp.

Yoneda, M., Kitano, H., Tanaka, H., Kawamura, K., Selvaraj, S. *et al.*, 2014. Temperature- and income resource availability- mediated variation in reproductive investment in a multiple-batch-spawning Japanese anchovy. *Marine Ecology Progress Series*, 516, 251-262.

Zwolinski, J., Stratoudakis, Y., Soares E., 2001. Intra-annual variation in the batch fecundity of sardine off Portugal. *Journal of Fish Biology*, 58 (6), 1633-1645.

Supplementary data

The following supplementary information is available online for the article:

A. Length-frequency distributions of *Etrumeus golanii* sampled in Crete

Fig. S1: Length frequency distributions of fish collected by the different gears. OTB: bottom trawl. PS: purse seine. PT: pelagic trawl. SB: beach seine. GTR: trammel net.

B. Macroscopic maturity stages

Table S1. *Etrumeus golanii*. Descriptions of macroscopic maturity stages adopted for *Etrumeus golanni*.

C. Simulation of the hydrodynamic-biogeochemical model

Fig. S2: Time series (2016-2019) of monthly mean SST and Chl-α (satellite and model-simulated). The lower panel shows the model simulated mesozooplankton concentration.